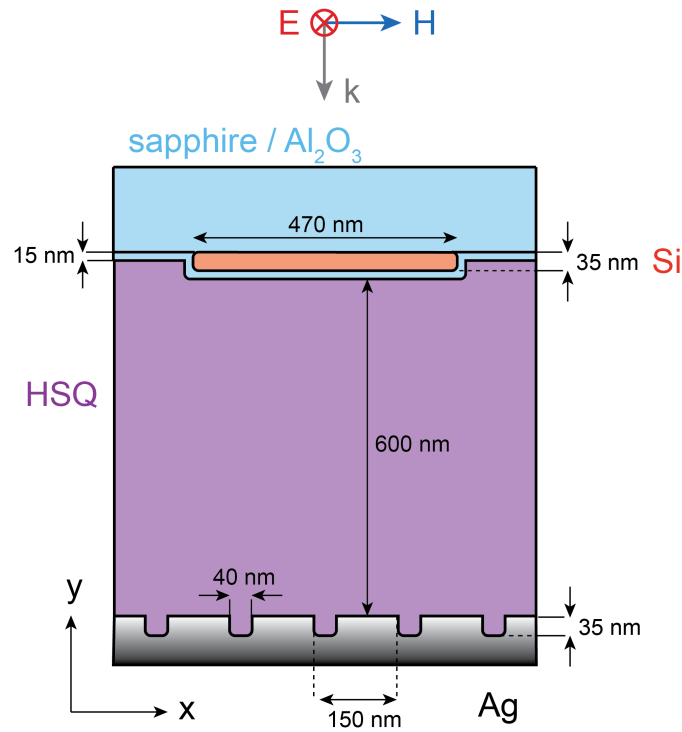


# Supporting Information: Metasurface mirrors for external control of Mie resonances

*Jorik van de Groep and Mark L. Brongersma*

Geballe Laboratory for Advanced Materials, Stanford University, 476 Lomita Mall, Stanford,  
California 94305, USA



**Figure S1.** Geometry used for FDTD simulations of the completed device (parallel groove orientation). The sapphire substrate is assumed to be semi-infinite and is simulated as having a non-dispersive index  $n = 1.77$ .

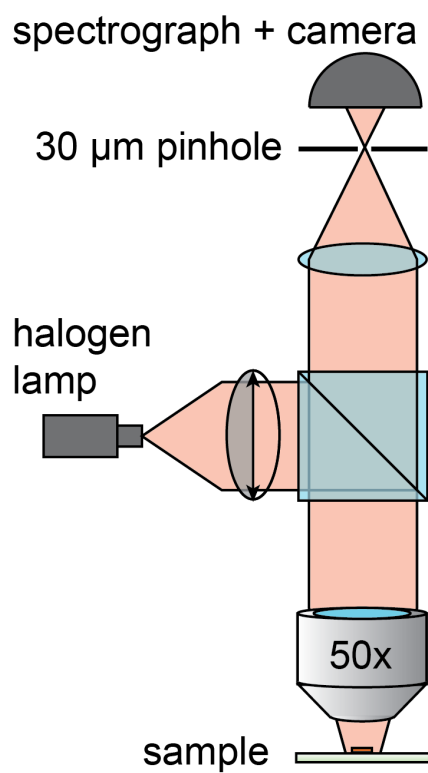


**Figure S2.** Schematic of confocal microscope used for bright-field backscattering measurements.

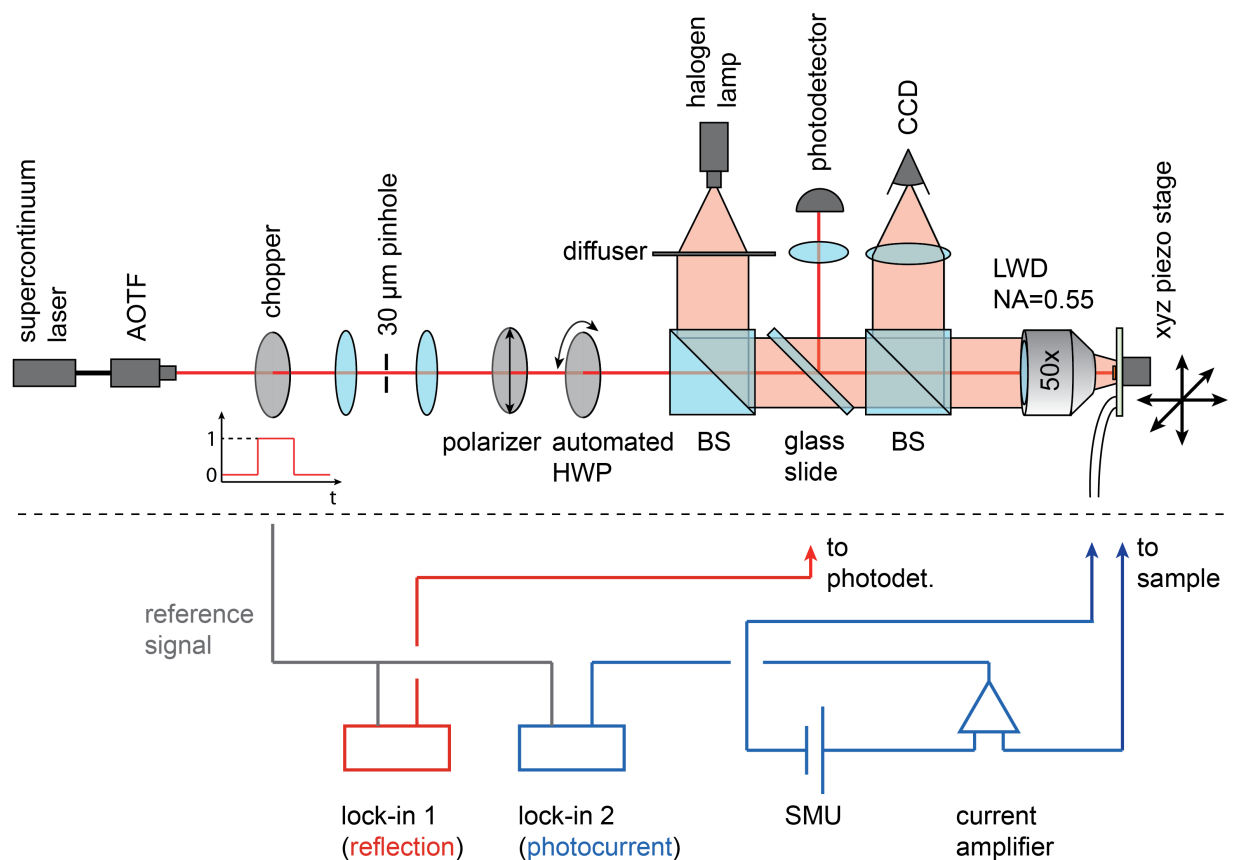


**Figure S3.** Schematic of optical (top) and electrical (bottom) components of the photocurrent setup. AOTF: acousto-optical tunable filter, HWP: half-wave plate, BS: beam splitter, CCD: charge-coupled device camera, LWD: long working distance, NA: numerical aperture, SMU: source-measure unit.

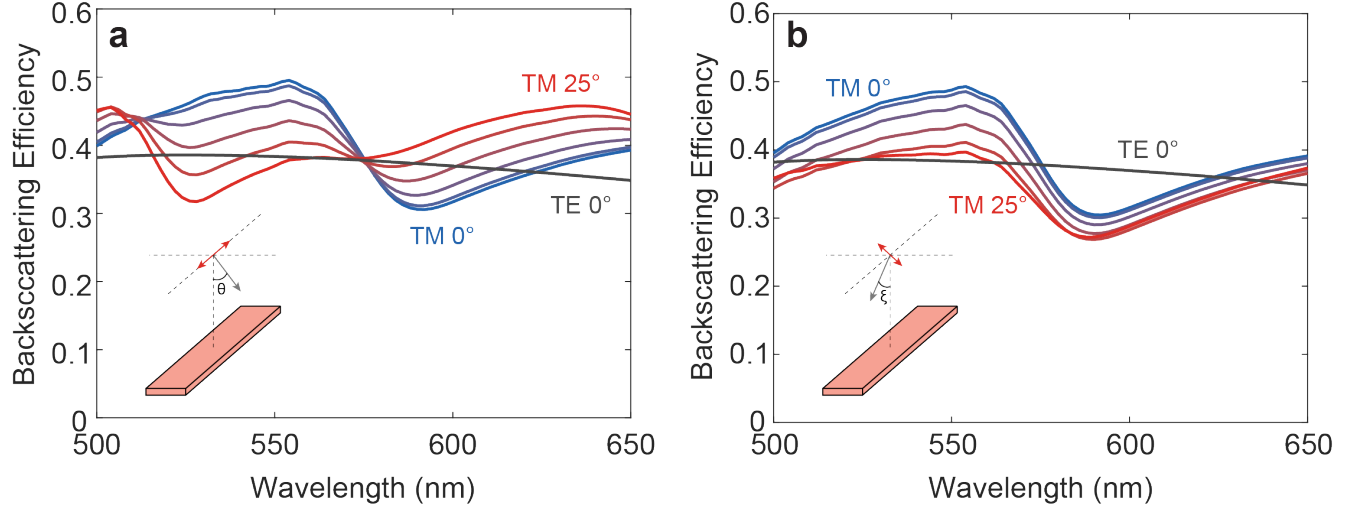


**Figure S4.** Resonant excitation for off-normal incident light. (a) Simulated backscattering efficiency of an infinitely long 490 nm x 35 nm Si NW on a sapphire substrate excited by a TM-polarized plane wave with angle  $\theta$  in the plane perpendicular to the NW axis (inset). The scattering efficiency for TE-polarization under normal incidence is also shown as a reference (gray). A reduced amplitude is observed for the Fano line shape around 575 nm for increasing angle of incidence, indicating reduced resonant excitation. (b) Simulated scattering efficiency for the same wire as in (a), excited by a TM polarized plane wave with angle  $\xi$  in the plane parallel to the NW axis. A small offset and reduction in amplitude is observed in the scattering efficiency, but no significant spectral shift.

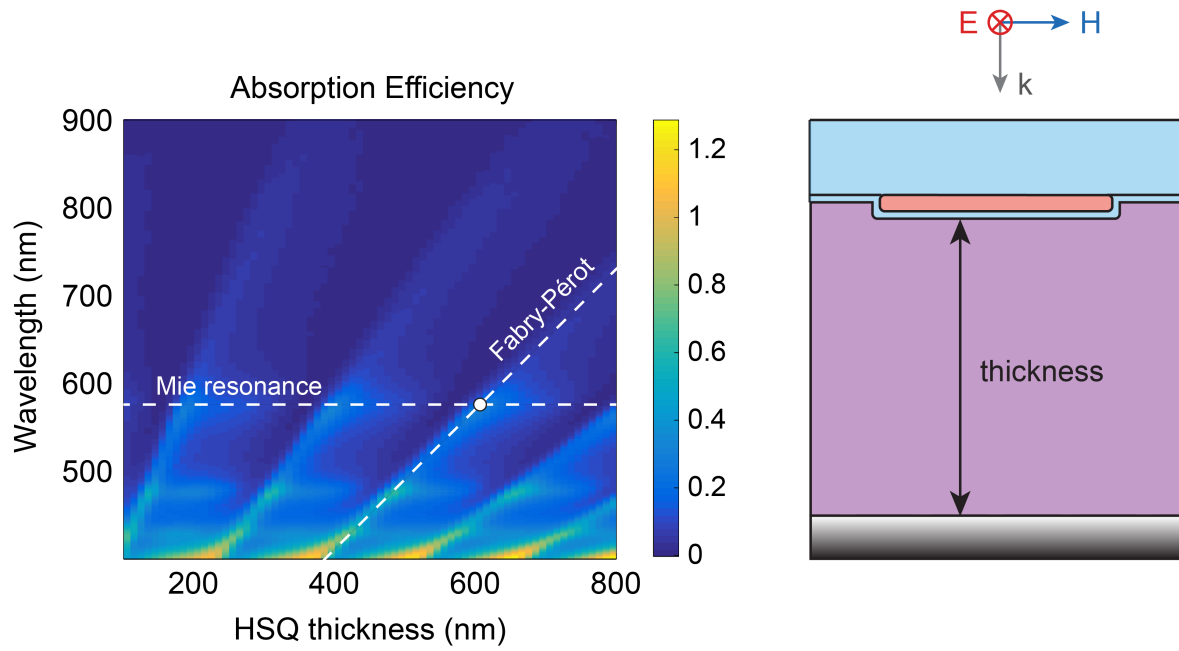


**Figure S5.** Optimization of HSQ thickness. Absorption efficiency (color) of Si NW ( $w = 470$  nm) spaced above a flat mirror using an HSQ spacer with thickness  $t$  (see schematic). Clear bands of high absorption efficiency can be observed as a result of the geometrical (Mie) resonance and Fabry-Pérot resonances. Enhanced absorption is observed when the resonances couple (e.g. at white dot). A thickness of 600 nm is used for the simulations of the completed device.

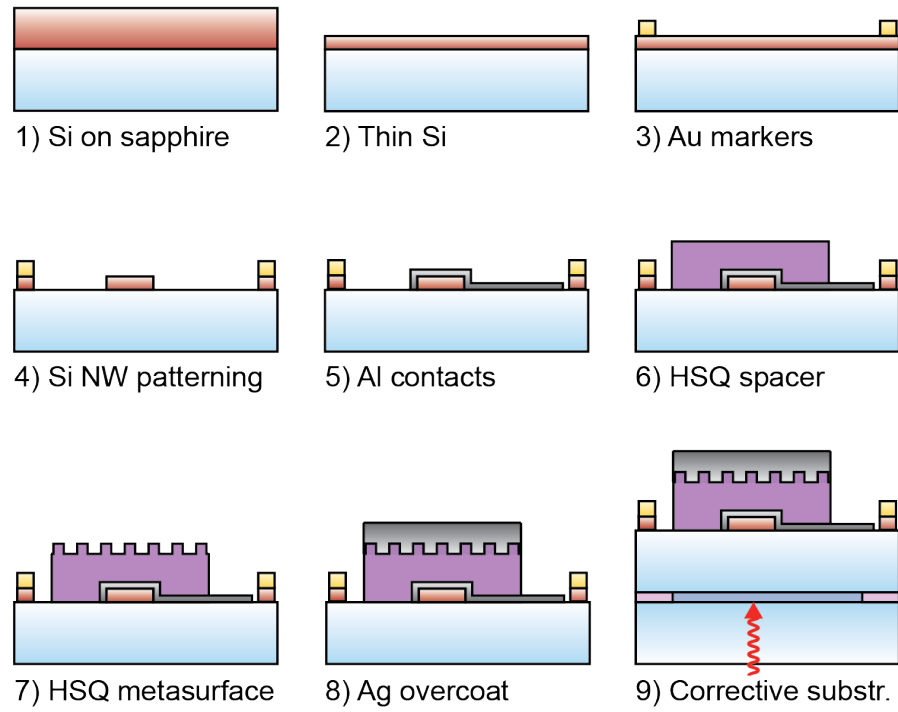


**Figure S6.** Schematic of the multi-step device fabrication process. See methods for details for each step, and additional steps not included in the schematic.

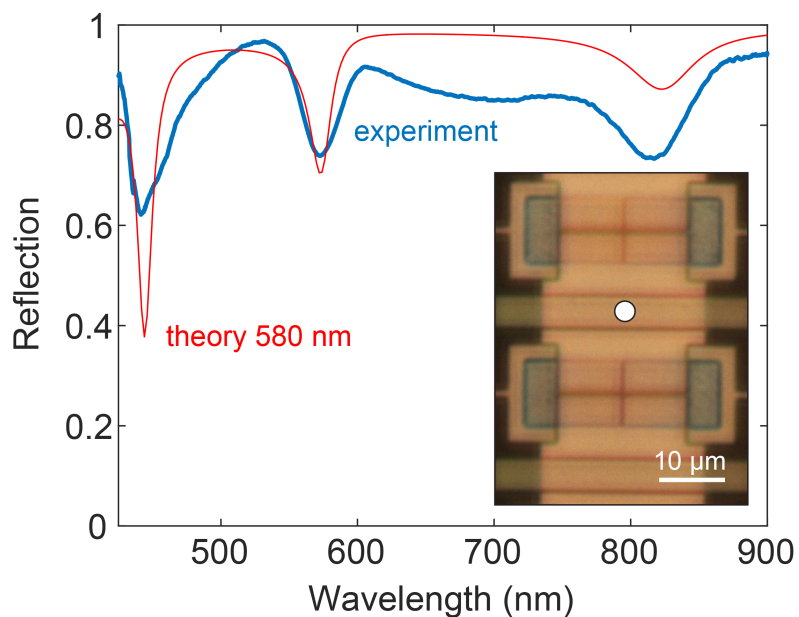


**Figure S7.** Reflection spectrum of continuous Si layer above the flat mirror. The thickness of the experimentally obtained HSQ spacer is calibrated by measuring the reflection spectrum of the continuous Si layer right next to the device (blue, see white dot in inset for location), and comparing it to the calculated spectrum (transfer-matrix method, red). Maximum absorption is observed at  $\lambda = 575$  nm.

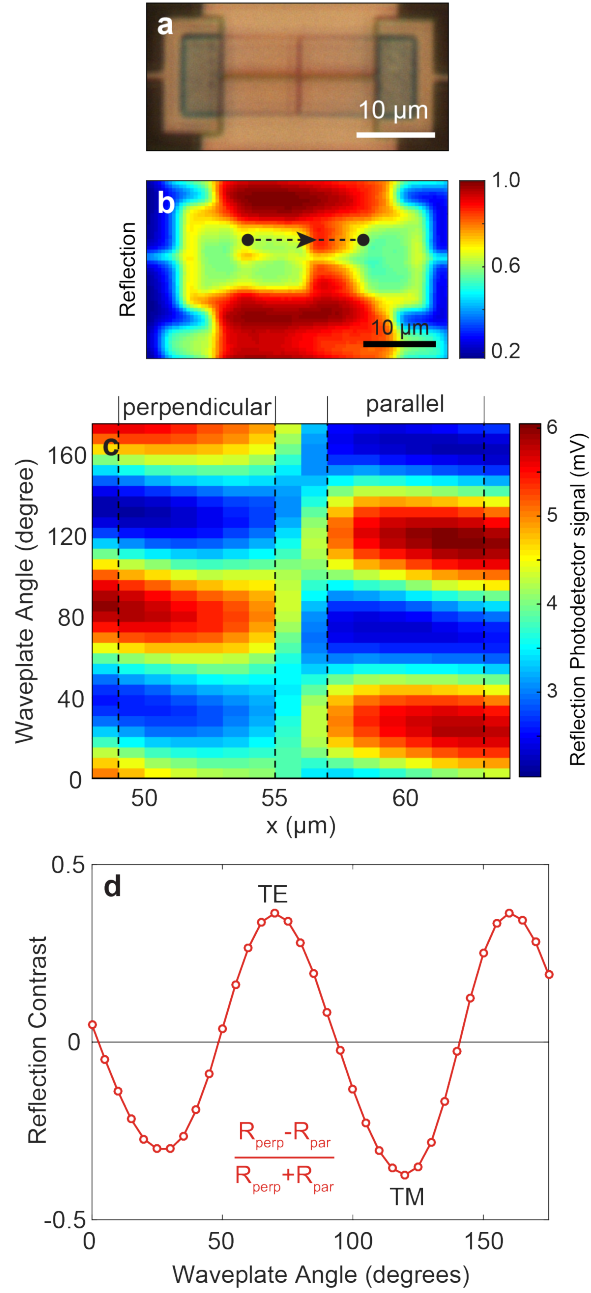


**Figure S8.** Polarization calibration for through-substrate illumination. (a) Optical microscope image of device through substrate. The two metamirror domains are clearly visible but with equal reflectance for unpolarized light. (b) Spatial reflection map for light ( $\lambda = 575 \text{ nm}$ ) polarized along wire axis. The perpendicular domain (left) shows lower reflection due to plasmonic losses, which can be used to calibrate the polarization at the position of the wire. The black dots and



dashed line indicates the line along which reflection of the metamirror is measured to obtain a line in c. (c) Reflection photodiode signal (color) as a function of position (see line in b) and half-wave plate angle. The spatial extent of the perpendicular and parallel domains is indicated above the plot and is used for spatial averaging. Clear contrast can be observed, which is maximum when the polarization is purely TM or TE. (d) Reflection contrast (defined in plot) as function of half-wave plate angle. The contrast follows a sinusoidal line shape and the angles that give most positive/negative contrast correspond to TE/TM polarization.

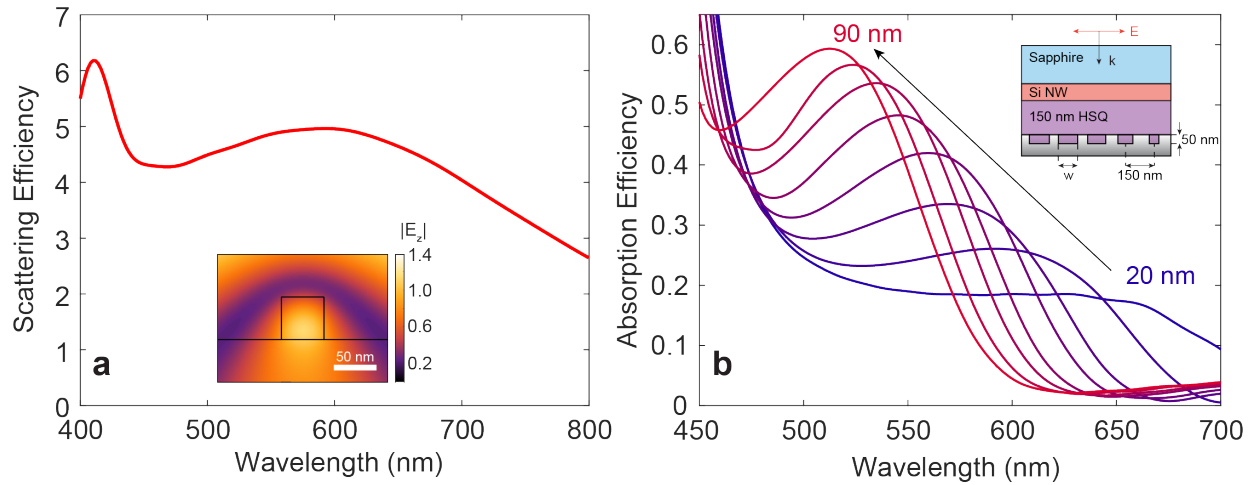


**Figure S9.** Controlling resonance wavelength using metamirror geometry. (a) Simulated scattering efficiency of a 50 nm x 50 nm Si NW on a sapphire substrate. A broad dipolar resonance is observed (see inset for field profile) spanning the entire visible spectral range. (b) Simulated absorption efficiency, showing strong spectral shifts for the resonant absorption as a result of the local metamirror geometry. Inset: schematic cross section along NW axis showing the simulated metasurface device. The base of the wire is spaced 150 nm above the metamirror, which has 50 nm deep grooves (150 nm period) with groove widths varying from 20 – 90 nm along the NW length.